

Supporting Information

Dines, J. P.*, E. Otárola-Castillo, P. Ralph, J. Alas, T. Daley, A. D. Smith, M. D. Dean*

*Correspondence: jdines@nhm.org, matthew.dean@usc.edu

A Materials and Methods

All original data and analytical code have been deposited in the Dryad Digital Repository (<http://dx.doi.org/10.5061/dryad.11111>).

Scanning bones and identifying landmarks

All bones were scanned with a NextEngine 3-dimensional Laser Scanner, returning tens of thousands of x, y, z points per bone. A pipeline was developed to sub-sample 962 evenly spaced and ordered points. The pipeline is graphically illustrated for pelvic bones (Fig. S3) and ribs (Fig. S4) separately. All original laser scans and the associated code for imposing landmarks has been made available on the Dryad Digital Repository (<http://dx.doi.org/10.5061/dryad.11111>).

Phylogenetic modeling

In addition to analyzing the data using phylogenetic least squares, we built an explicit phylogenetic model to test for correlated evolution of testes size and bone centroid size, which we now describe in detail. The sample-specific morphological data (Tables S1–S2) were placed on a cetacean phylogeny constructed from 45 nuclear loci, transposons, and mitochondrial genomes (19). The logarithms of all values were then modeled as evolving on the tree as correlated Gaussian traits, accounting for intraspecific and intraindividual variation and missing data. Priors were placed on the 16 covariances of this model (including separate parameters for within-species variation), and the posterior distribution was evaluated using Markov chain Monte Carlo. All associated code for running these analyses have been made available on the Dryad Digital Repository (<http://dx.doi.org/10.5061/dryad.11111>).

Correlated trait evolution

It is clear that cetacean testes size, rib bone size, and pelvic bone size should evolve in a correlated manner over evolutionary time due to their common correlation with total body size (which varies considerably from dolphins to baleen whales); to discover whether pelvic bone and testes size changes are correlated after accounting for body size changes requires a joint model of their evolution along the phylogeny.

The general framework we used to analyze these data is similar to those used in Revell and Collar (37) and Harmon et al. (38), modified to account for within-species variation, missing data, and measurement of different variables at the species and/or individual level. We do not account for uncertainty in the phylogeny, as suggested by Huelsenbeck and Rannala (39), since it is unclear how much we should let body length and bone size influence branch lengths, and we do not think that uncertainty in phylogeny will be a significant confounding factor.

Specifically, we have the following information about a number of individual whales: species, sex, body length, and the sizes of the right and left pelvic and anterior-most pair of vertebral rib bones (although some of the measurements are missing). Furthermore, for each species, we have maximum recorded male body length and testes mass.

There are three levels of variation: between species (i.e. changes across branches in the phylogeny), between individuals in a species, and between left and right pairs of bones in each individual. These can be visually put into a common framework by labeling the species tips of the phylogeny as the “species

mean”, attaching additional edges to each species for each observed individual of that species (“individual edges”). Trait differences are then written as the sum over trait changes along intervening edges. For instance, the difference between a particular left rib size and the species mean rib size is the sum of the difference between the rib size and that individual’s mean rib sizes and the difference between that individual’s mean and the species mean rib size. Differences between two samples from different species include terms for both individuals’ deviations from their species means, as well as changes in species mean trait values along each edge of the phylogeny that separates the two species. The species-level observation of testes size is treated as direct observation of the species mean; since we do not observe testes size in individuals, omitting modeling the observation error should not affect the analysis.

The inclusion of within-individual variation suggests attaching two additional branches of a third type to each individual’s tip; however, it simplifies the analysis to instead treat left rib and right rib size as separate traits that evolve on the phylogeny, but to assume that their evolution is perfectly correlated except on edges corresponding to intraspecific variation (and similarly for left and right pelvic size).

We then model the observed set of trait values as resulting from correlated changes across this ramified phylogeny, with different sets of parameters for each of the three types of edges. Concretely, we take logarithms of all quantitative traits, and model their evolution as a correlated Brownian motion. We write these six traits as

$$L = \log(\text{body length}), \quad (1)$$

$$T = \log(\text{testes volume}), \quad (2)$$

$$P^R = \log(\text{right pelvic centroid size}), \quad (3)$$

$$P^L = \log(\text{left pelvic centroid size}), \quad (4)$$

$$R^R = \log(\text{right rib centroid size}), \quad (5)$$

$$R^L = \log(\text{left rib centroid size}), \quad (6)$$

and now need to specify our parameterization of the covariance across each type of branch.

Species differences

First consider the difference of two species means across an internal (species) edge of length t in the phylogeny. Writing $X_0 = (L_0, T_0, R_0^R, R_0^L, P_0^R, P_0^L)$ for the mean trait values of the ancestor, and $X_t = (L_t, T_t, R_t^R, R_t^L, P_t^R, P_t^L)$ for the mean trait values of the descendant, our model is that $X_t = X_0 + \sqrt{t}AZ$, with Z independent standard Gaussians and A_t the matrix given here:

$$\begin{bmatrix} L_t \\ T_t \\ R_t^R \\ R_t^L \\ P_t^R \\ P_t^L \end{bmatrix} = \begin{bmatrix} L_0 \\ T_0 \\ R_0^R \\ R_0^L \\ P_0^R \\ P_0^L \end{bmatrix} + \sqrt{t} \begin{bmatrix} \sigma_L & 0 & 0 & 0 \\ \delta_T & \beta_T & 0 & 0 \\ \delta_R & \beta_R & \sigma_R & 0 \\ \delta_R & \beta_R & \sigma_R & 0 \\ \delta_P & \beta_P & 0 & \sigma_P \\ \delta_P & \beta_P & 0 & \sigma_P \end{bmatrix} \begin{bmatrix} Z_1 \\ Z_2 \\ Z_3 \\ Z_4 \end{bmatrix} \quad (7)$$

In this parameterization, the covariance matrix of the trait differences $(X_t - X_0)$ is $\Sigma_t = A_t A_t^T$; effectively, we are parameterizing the covariance matrix through its Cholesky decomposition, subject to the constraint that left and right bone size changes are perfectly correlated. A direct parameterization of Σ_t is

difficult to optimize over due to the complex constraints imposed by the condition that Σ_t be nonnegative definite; the constraints on A_t are only that the diagonal elements are positive (40).

Individual variation

We use a similar parameterization for within-species and within-individual variation. If the species mean trait values are $X_S = (L_S, T_S, R_S^R, R_S^L, P_S^R, P_S^L)$ and the trait values of an individual are $X_I = (L_I, T_I, R_I^R, R_I^L, P_I^R, P_I^L)$, then we write $X_I = X_S + BW$, again with W independent standard Gaussians, and B parameterized by

$$\begin{bmatrix} L_I \\ T_I \\ R_I^R \\ R_I^L \\ P_I^R \\ P_I^L \end{bmatrix} = \begin{bmatrix} L_S \\ T_S \\ R_S^R \\ R_S^L \\ P_S^R \\ P_S^L \end{bmatrix} + \begin{bmatrix} \zeta_L & 0 & 0 & 0 & 0 \\ - & - & - & - & - \\ \eta_R & \zeta_R & \omega_R & 0 & 0 \\ \eta_R & \zeta_R & -\omega_R & 0 & 0 \\ \eta_P & 0 & 0 & \zeta_P & \omega_P \\ \eta_P & 0 & 0 & \zeta_P & -\omega_P \end{bmatrix} \begin{bmatrix} W_1 \\ W_2 \\ W_3 \\ W_4 \\ W_5 \end{bmatrix} \quad (8)$$

Here the row of B corresponding to testes size is omitted because we do not observe testes size in individuals; this will not enter the analysis. In this form, ζ_R^2 parameterizes the within-species variance of individual mean rib sizes, and ω_R^2 parameterizes the variance of rib sizes within an individual.

Note that this effectively assumes that within-species variation is of the same magnitude for each species, and furthermore no substructure within each species. If these are not good assumptions, one could add individual-level random effects (for instance); but we did not see evidence that this was necessary.

Mean-centering the data

Above we have given a complete model for correlated trait evolution along a phylogeny, including within-species variation, given the trait values at the root. It is usual in phylogenetics to compute the independent contrasts – effectively, performing a linear transformation of the tip values that (a) renders them independent of the root value and (b) results in jointly independent values. The second property is merely a computational convenience, while the first property is essential. This would be straightforward in this model if the species-level matrices A and the individual-level matrices B were jointly diagonalizable (as in 37).

Fortunately, if we subtract any unbiased estimate of the root value, we obtain values that do not depend on the root value. To see this, let X_{ik} denote the matrix of trait values at the tips, with rows corresponding to individuals, and let M_{ik} be a matrix whose columns sum to 1, so that $\bar{X}_k = \sum_i M_{ik} X_{ik}$ is an estimate of the k^{th} trait at the root. Also write dX_e for the vector of trait differences across edge e in the tree, and X_ρ for the trait values at the root, so that $X_i = X_\rho + \sum_{e \in \rho \rightarrow i} dX_e$, where $\{e \in \rho \rightarrow i\}$ are the edges in the path from the root to tip i . Then the centered observations $\tilde{X}_{ik} := X_{ik} - \bar{X}_k$ do not depend on X_ρ : if we assign weight M_{ek} to each edge e proportional to the weights that M assigns to tips below it, i.e. $M_{ek} = \sum_{i: e \in \rho \rightarrow i} M_{ik}$, then

$$\tilde{X}_{ik} = \sum_{e \in \rho \rightarrow i} dX_{ek} - \sum_e M_{ek} dX_{ek}, \quad (9)$$

which does not depend on the trait values at the root.

For the weights M that estimate the trait values at the root, we use the “phylogenetic mean” (41), calculated independently for each trait, using fairly short values for the branch lengths of the individual edges estimated from within-species variances, as that should be fairly close to the minimum-variance estimator of the root values. Note that the columns of M are *not* identical, due to the irregular pattern of missing data.

Likelihood computation

So far, we have given the covariance matrices for differences in trait values across each edge (dX_e in the notation above), have assumed that these values are independent for each edge, and we now need to convert this to a covariance matrix for the data we do actually observe, mean-centered as described above. Since the mean-centered data are by assumption centered Gaussian, this is all we need to compute the likelihood of the data, given the covariance parameters in (7) and (8).

Suppose that U is a n -dimensional Gaussian vector with covariance matrix Σ (the edge differences dX_e in some order), and $V = QU$ is a linear transformation of U by the matrix Q (the observed data), then V is also Gaussian, with covariance matrix $\tilde{\Sigma} = Q\Sigma Q^T$. Again, we have Σ but would like $\tilde{\Sigma}$. Note above in equation (9) that the mean-centered data is a linear transformation of the differences across edges, so that it is only a matter of bookkeeping to find the matrix C corresponding to this transformation. However, the matrix $C\Sigma C^T$ will be singular, since mean-centering reduces the number of degrees of freedom (here by four, as we subtract four trait means). A simple computational way around this is to take Q to be a projection matrix into the column space of C , and to transform both the data and the covariance matrix by Q as above. Since weights M assign zero influence to missing values in the data, Q will automatically omit such missing values: the columns of Q corresponding to missing values will be zero. (Another choice would be to let P be the matrix that drops one individual, and take $Q = PC$; but this is less numerically robust and becomes trickier in the presence of missing data.)

Now that we have the covariance function, the computation is standard: recalling that Y is the transformed, mean-centered data and $\tilde{\Sigma}(\theta)$ is the covariance matrix of Y , which depends on the parameters θ ,

$$\mathcal{L}(Y|\theta) = \frac{1}{\left(2\pi \det \tilde{\Sigma}(\theta)\right)^{n/2}} \exp\left(-\frac{1}{2}Y^T \tilde{\Sigma}(\theta)Y\right). \quad (10)$$

To compute this, we do the following:

1. Compute the full covariance matrix $\Sigma(\theta)$ from the parameters θ .
2. Compute $\tilde{\Sigma}(\theta) = Q\Sigma Q^T$ (note that Q does not depend on the parameters).
3. Compute $\det \tilde{\Sigma}(\theta)$ and $Y^T \tilde{\Sigma}(\theta)Y$ from the Cholesky decomposition of $\tilde{\Sigma}(\theta)$ (found numerically).

The first step is simplified by precomputation of appropriate matrices to place the parameters into the appropriate slots of Σ .

Priors and Bayesian methods

Now that we have an easily computable likelihood function, we put priors on each of the parameters, and estimate the posterior distribution of the parameters given the data by a standard random-walk Markov chain Monte Carlo (MCMC) (as implemented in the `mcmc` package (42) in R, R Core Team (43)).

Roughly speaking, the parameters controlling variances are σ_L , β_T , σ_R , σ_P , ζ_L , ζ_R , ω_R , ζ_P , and ω_P . Those controlling covariances are δ_T , δ_R , δ_P , β_R , β_P , η_R , and η_P . We placed independent zero-mean Gaussian priors on all parameters, conditioning the variance parameters to be nonzero. Based on examination of variability in various traits, we set the prior standard deviations of σ_L , β_T , β_P , σ_R , σ_P , and ζ_L to 3, the prior standard deviations of δ_T , δ_R , and δ_P to 1, and the prior standard deviations of ζ_R , ω_R , ζ_P , ω_P , β_R , η_R , and η_P to 0.1.

Proportion of changes explained by mating ecology

It is of interest to estimate what proportion of changes in pelvic bone size are due to shifts in mating ecology, relative to other causes, e.g. changes in species mean body length or random drift. Under the model described above (equation (7)):

$$dP = \delta_P dZ_1 + \beta_P dZ_2 + \sigma_P dZ_4, \quad (11)$$

where each dZ are independent white noise terms, each having the same variance. dZ_1 corresponds to normalized changes in body length, dZ_2 corresponds to normalized changes in testes size after accounting for changes in body length, and dZ_4 is pelvic-specific noise. Therefore,

$$\frac{\beta_P}{\delta_P + \beta_P + \sigma_P} \quad (12)$$

is a measure of the proportion of changes in pelvic bone size changes that are accounted for by changes in testes size. There is an analogous measure for ribs.

Running the MCMC sampler

To carefully check that our results were not affected by patterns of missing data, we ran an MCMC sampler to estimate the posterior distribution of the above parameters on three datasets: **(a)** all bones from adult male cetaceans, **(b)** all bones from adult female cetaceans, and **(c)** all bones from adult male cetaceans for which we had data from both ribs and pelvic bones. The dataset (c) is a subset of (a); these differed primarily because the ribs of most baleen whales were too large to scan on available equipment, so comparisons between ribs and pelvic bones in dataset (a) could potentially be misleading. As described below, results from (c) did not differ substantially from (a), so we present the results of (a) in the main text. Each dataset was run using the same pipeline, by simply setting the relevant observations to missing.

In each case, the MCMC sampler was run for a total of 500,000 iterations, the first 20,000 of which were discarded as burn-in, at which point it was apparent from trace plots that convergence had been reached.

Results

Here we present additional results from the analysis of correlation trait evolution on the cetacean phylogeny described above.

Full dataset for males

The summary statistics of the estimated posterior distributions for the parameters are given in table S3. Taking posterior mean values, we see that $0.07/(0.47+0.07+0.07) = 0.11$ of the changes in pelvic bone size is derivable from shifts in testes size after removing the effects of length shifts, an equal quantity is pelvic-specific noise, and only 0.78 comes from changes in body length.

The correlation matrix for changes along a branch at the posterior mean parameter values is

$$\begin{bmatrix} 1.00 & 0.95 & 1.00 & 0.98 \\ 0.95 & 1.00 & 0.94 & 0.97 \\ 1.00 & 0.94 & 1.00 & 0.98 \\ 0.98 & 0.97 & 0.98 & 1.00 \end{bmatrix} \begin{matrix} \leftarrow (\text{length}) \\ \leftarrow (\text{testes}) \\ \leftarrow (\text{ribs}) \\ \leftarrow (\text{pelvis}) \end{matrix} \quad (13)$$

The correlations are high, but this is due to shared correlations with length. We can remove this effect by calculating the correlation in trait changes after subtracting off the expected trait change based on body length change. (Since the trait changes are multivariate Gaussian, this is equivalent to the correlation matrix for the trait changes conditional on the length change, and does not depend on the value of the length change.) This can be thought of as the correlation in the residuals of trait changes after regressing out body length change, or as the correlation between trait changes on a hypothetical branch over which body length does not change. This results in following posterior mean correlation matrix:

$$\begin{bmatrix} 1 & r_{TR} & r_{TP} \\ r_{TR} & 1 & r_{RP} \\ r_{TP} & r_{RP} & 1 \end{bmatrix} = \begin{bmatrix} 1.00 & 0.07 & 0.67 \\ 0.07 & 1.00 & 0.05 \\ 0.67 & 0.05 & 1.00 \end{bmatrix} \begin{matrix} \leftarrow (\text{testes}) \\ \leftarrow (\text{rib}) \\ \leftarrow (\text{pelvis}) \end{matrix} \quad (14)$$

We can furthermore postprocess the MCMC samples from posterior distribution to obtain marginal posterior distributions for the three correlations. These are shown in figure 4 in the main text; and summary statistics are shown in table S4.

The correlation matrix for intraspecific variation (i.e. for differences of individuals to the species mean) at the posterior mean parameter values is

$$\begin{bmatrix} 1.00 & 0.39 & 0.39 & 0.13 & 0.13 \\ 0.39 & 1.00 & 0.57 & 0.05 & 0.05 \\ 0.39 & 0.57 & 1.00 & 0.05 & 0.05 \\ 0.13 & 0.05 & 0.05 & 1.00 & 0.96 \\ 0.13 & 0.05 & 0.05 & 0.96 & 1.00 \end{bmatrix} \begin{matrix} \leftarrow (\text{length}) \\ \leftarrow (\text{right ribs}) \\ \leftarrow (\text{left ribs}) \\ \leftarrow (\text{right pelvis}) \\ \leftarrow (\text{left pelvis}) \end{matrix} \quad (15)$$

It is interesting to note that there is more intraspecific variation in pelvic bones than ribs (table S3, $\zeta_P > \zeta_R$), despite ribs being typically larger, but that the two pelvic bones of an individual tend to be more similar to each other (relative to the species mean) than are the two ribs.

Males, complete data only

The summary statistics of the estimated posterior distributions for the parameters are given in table S5.

The correlation matrix for changes along a branch at the posterior mean parameter values is

$$\begin{bmatrix} 1.00 & 0.97 & 1.00 & 1.00 \\ 0.97 & 1.00 & 0.97 & 0.98 \\ 1.00 & 0.97 & 1.00 & 1.00 \\ 1.00 & 0.98 & 1.00 & 1.00 \end{bmatrix} \begin{matrix} \leftarrow (\text{length}) \\ \leftarrow (\text{testes}) \\ \leftarrow (\text{ribs}) \\ \leftarrow (\text{pelvis}) \end{matrix} \quad (16)$$

As above, removing the effects of length changes results in following posterior mean correlation matrix:

$$\begin{bmatrix} 1 & r_{TR} & r_{TP} \\ r_{TR} & 1 & r_{RP} \\ r_{TP} & r_{RP} & 1 \end{bmatrix} = \begin{bmatrix} 1.00 & 0.06 & 0.63 \\ 0.06 & 1.00 & 0.04 \\ 0.63 & 0.04 & 1.00 \end{bmatrix} \begin{matrix} \leftarrow (\text{testes}) \\ \leftarrow (\text{rib}) \\ \leftarrow (\text{pelvis}) \end{matrix} \quad (17)$$

As above, we obtain marginal posterior distributions for the three correlations. Summary statistics are shown in table S6, and distributions are shown in figure S7.

The correlation matrix for intraspecific variation (i.e. for differences of individuals to the species mean) at the posterior mean parameter values is

$$\begin{bmatrix} 1.00 & 0.41 & 0.41 & 0.11 & 0.11 \\ 0.41 & 1.00 & 0.58 & 0.05 & 0.05 \\ 0.41 & 0.58 & 1.00 & 0.05 & 0.05 \\ 0.11 & 0.05 & 0.05 & 1.00 & 0.96 \\ 0.11 & 0.05 & 0.05 & 0.96 & 1.00 \end{bmatrix} \begin{matrix} \leftarrow (\text{length}) \\ \leftarrow (\text{right ribs}) \\ \leftarrow (\text{left ribs}) \\ \leftarrow (\text{right pelvis}) \\ \leftarrow (\text{left pelvis}) \end{matrix} \quad (18)$$

Full dataset for females

As above, the summary statistics of the estimated posterior distributions for the parameters are given in table S7.

The correlation matrix for changes along a branch at the posterior mean parameter values is

$$\begin{bmatrix} 1.00 & 0.50 & 0.98 & 0.82 \\ 0.50 & 1.00 & 0.53 & 0.82 \\ 0.98 & 0.53 & 1.00 & 0.82 \\ 0.82 & 0.82 & 0.82 & 1.00 \end{bmatrix} \begin{matrix} \leftarrow (\text{length}) \\ \leftarrow (\text{testes}) \\ \leftarrow (\text{ribs}) \\ \leftarrow (\text{pelvis}) \end{matrix} \quad (19)$$

As above, removing the effects of length changes results in following posterior mean correlation matrix:

$$\begin{bmatrix} 1 & r_{TR} & r_{TP} \\ r_{TR} & 1 & r_{RP} \\ r_{TP} & r_{RP} & 1 \end{bmatrix} = \begin{bmatrix} 1.00 & 0.22 & 0.82 \\ 0.22 & 1.00 & 0.18 \\ 0.82 & 0.18 & 1.00 \end{bmatrix} \begin{matrix} \leftarrow (\text{testes}) \\ \leftarrow (\text{rib}) \\ \leftarrow (\text{pelvis}) \end{matrix} \quad (20)$$

We can furthermore postprocess the MCMC samples from posterior distribution to obtain marginal posterior distributions for the three correlations. These are shown in figure S9, and summary statistics are shown in table S8.

The correlation matrix for intraspecific variation (i.e. for differences of individuals to the species mean) at the posterior mean parameter values is

$$\begin{bmatrix}
 1.00 & 0.26 & 0.26 & 0.21 & 0.21 \\
 0.26 & 1.00 & 0.92 & 0.05 & 0.05 \\
 0.26 & 0.92 & 1.00 & 0.05 & 0.05 \\
 0.21 & 0.05 & 0.05 & 1.00 & 0.91 \\
 0.21 & 0.05 & 0.05 & 0.91 & 1.00
 \end{bmatrix}
 \begin{matrix}
 \leftarrow (\text{length}) \\
 \leftarrow (\text{right ribs}) \\
 \leftarrow (\text{left ribs}) \\
 \leftarrow (\text{right pelvis}) \\
 \leftarrow (\text{left pelvis})
 \end{matrix}
 \quad . \quad (21)$$

Supplementary figures and tables

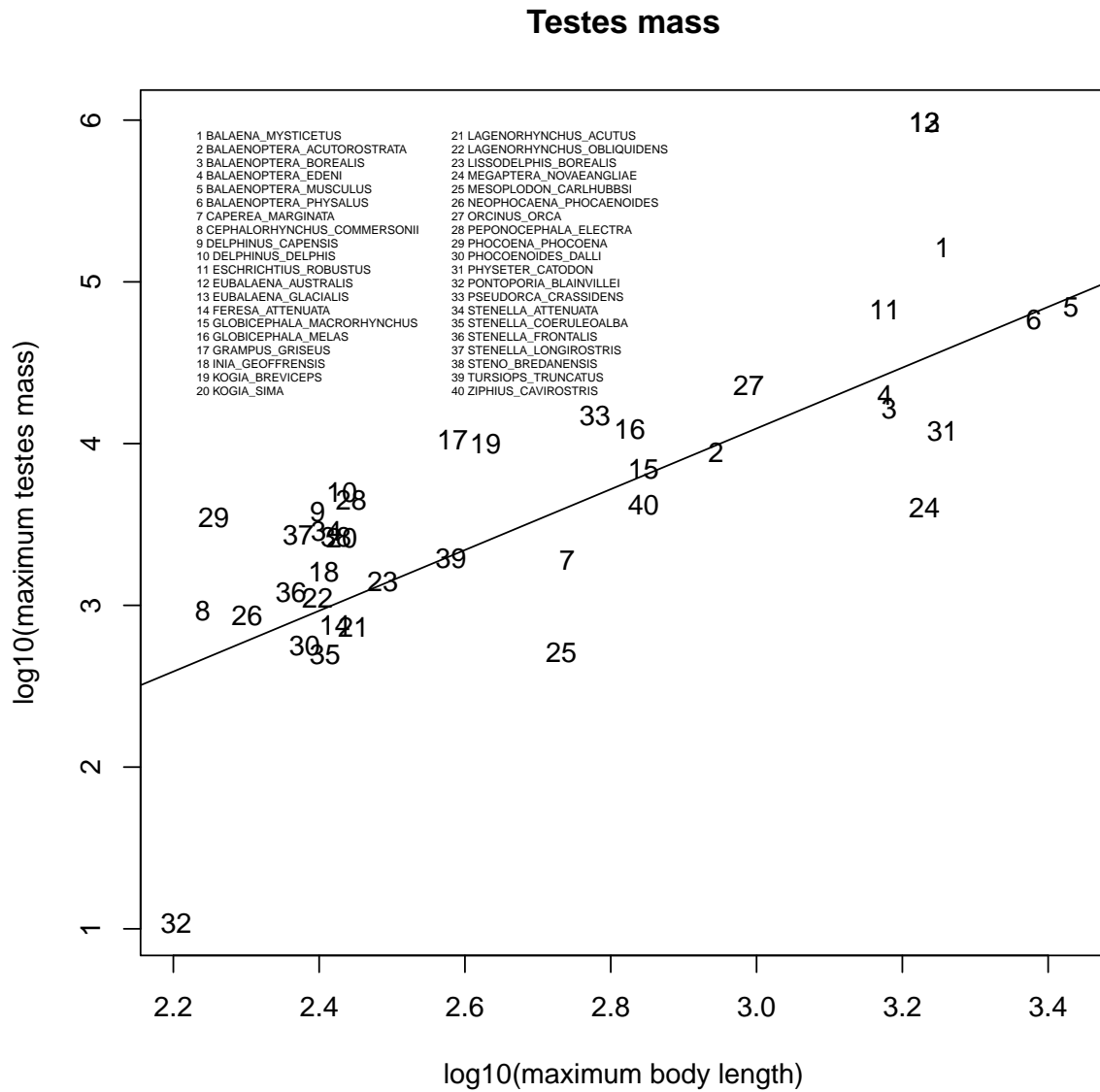


Figure S1. The regression of maximal recorded testis size onto maximal recorded body mass. The regression was drawn using the GLS procedure in the R package NLME, with a correlation structure that accounted for phylogenetic relatedness (44), using the corPagel procedure in the R package APE (45). The phylogenetic residuals were used as a measure of relative testes size.

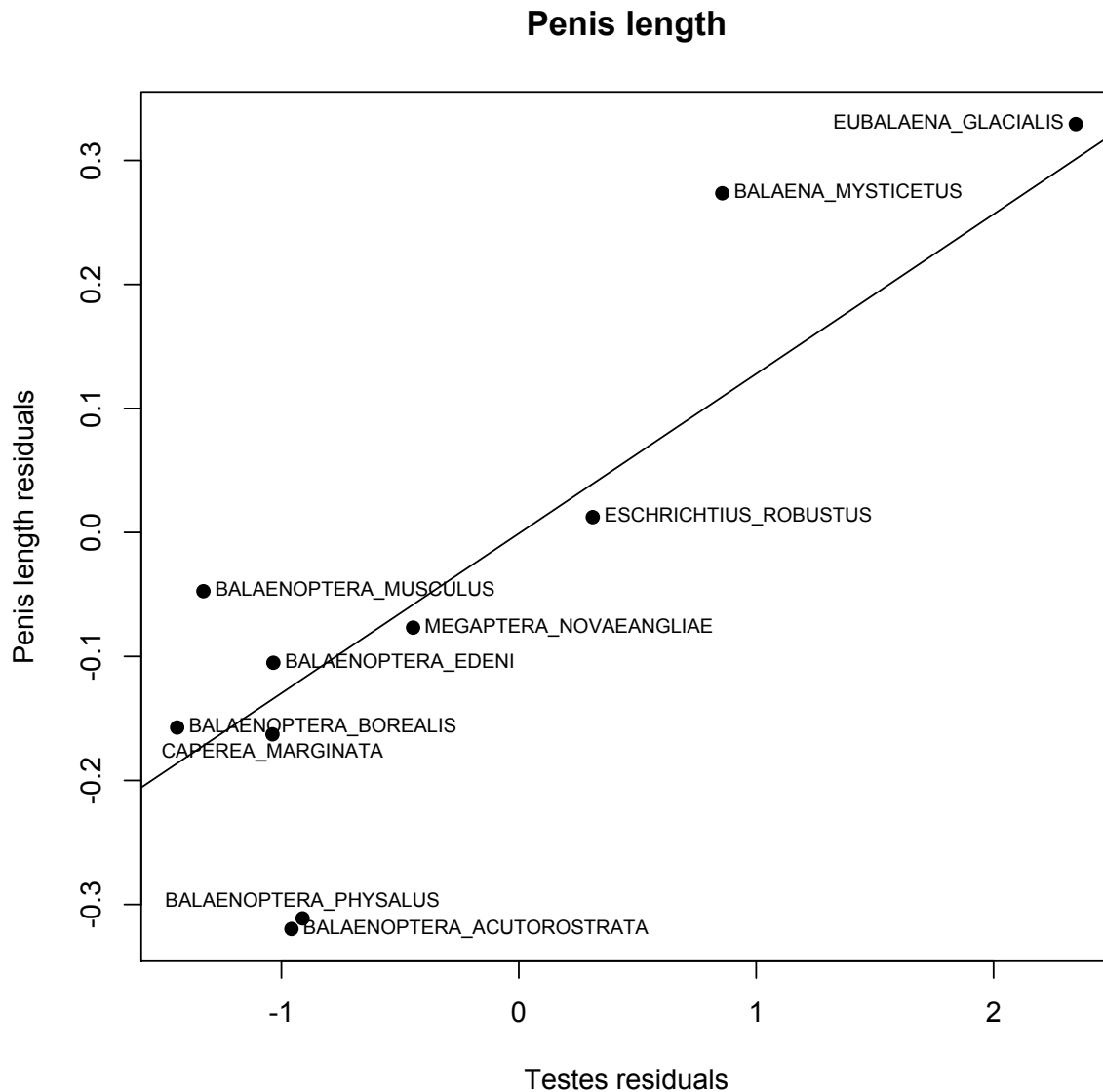


Figure S2. Whale species with relatively large testes have relatively long penises. Two separate regressions, each drawn using the GLS procedure in the R package NLME and a correlation structure accounting for phylogenetic relatedness (44) using the corPagel procedure in the R package APE (45), were drawn to derive the residuals of penis length onto body mass, and testes mass onto body mass. A third phylogenetic regression (pictured here) was used to test the correlation of residual penis length with residual testis mass. Raw data taken from Table 2 of (7), and analyzed in the phylogenetic framework of (19).

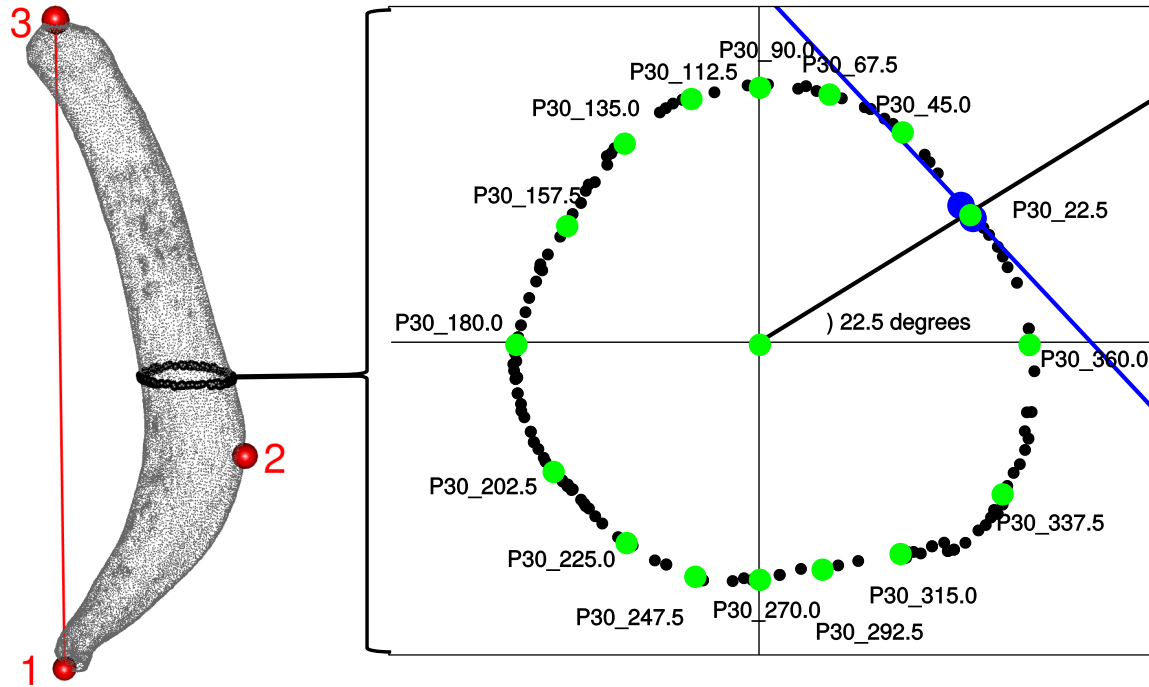


Figure S3. A series of tools in computational geometry were deployed to define landmarks from pelvic bone scans. First, the two furthest points apart were found to represent the most posterior and most anterior points (point 1 and 3). The entire point cloud was transformed so that point 1 was $x=0, y=0, z=0$, and point 3 was $x=0, y=0$, with some positive value of z . A new z -axis was drawn between point 1 and 3 (red line), and the point furthest from this line found (point 2), and the entire point cloud transformed so that point 2 was $x=\text{some positive value}, y=0, z=\text{some positive value}$. After this initial transformation, we sampled points that fell within the most posterior 0.5% of the z axis, the most anterior 0.5% of the z axis, or the middle 0.5% of the z axis (typically, several hundred points sampled each region), and calculated the centroid of their respective convex hulls. This second transformation accounted for variation in the placement of the first three points. Then, 60 evenly-spaced slices of points were sampled along the z axis, where each slice thickness was 0.5% the length of the z -axis. One slice appears in the right panel as an example. For each slice, the midpoint of the convex hull was calculated (green point in middle of right panel). Then, moving in increments of 22.5 degrees from the x -axis (only the first increment shown in detail), we determined the two points straddling the line extending from the centroid (two points shown in blue, one slightly obscured, with connecting line drawn in blue). A landmark was defined as the intersection of the black and blue lines (green point) and named according to its slice (i.e., P30) and its angle from the x -axis (i.e., 22.5). Only P30_22.5 is shown in detail: the other green points are shown for completeness. All green points correspond to the green points shown in Fig. 1C of the manuscript. Only the green points were included in downstream analyses; all other points were discarded.

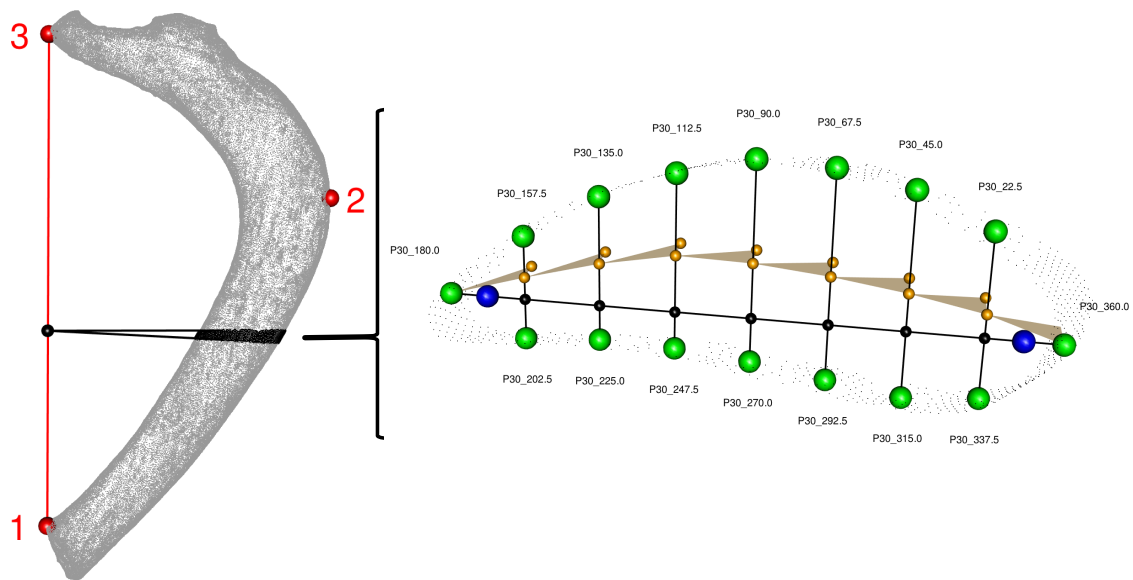


Figure S4. A series of tools in computational geometry were deployed to define landmarks from rib bone scans. First, all points were initially transformed according to the same three initial points described in Fig. S3 for pelvic bones. Then, a fulcrum (black sphere) was placed 1/3 up the length of the z-axis, and the bone scan divided into 60 slices of equal angle from that fulcrum. For each slice (the 30th slice shown as an example in right panel), the centroid of the convex hull of the 20% most medial points (leftmost blue sphere) and 20% most lateral points (rightmost blue sphere) points was used to draw a line. We identified the point on that line which was closest to a point in the original scan (rightmost/leftmost green spheres, right panel). This line was then divided evenly (black spheres) and lines perpendicular to the black spheres computed. All points from the original scan within a certain distance to the perpendicular lines were found, projected onto the perpendicular line and the midpoint computed (orange spheres on perpendicular lines, right panel). The orange sphere was projected onto the plane parallel to the figure to find a third point with which to draw a plane (indicated by orange triangles, right panel). Those orange triangles allowed us to divide the bone into anterior and posterior halves and to account for complex curvatures. The corresponding green spheres on the perpendicular lines were determined as done for the medial and lateral green spheres. All green spheres are named as described in Fig. S3, and correspond to the green spheres shown in Fig. 1D of the manuscript. Only the green spheres were included in downstream analyses; all other points were discarded.

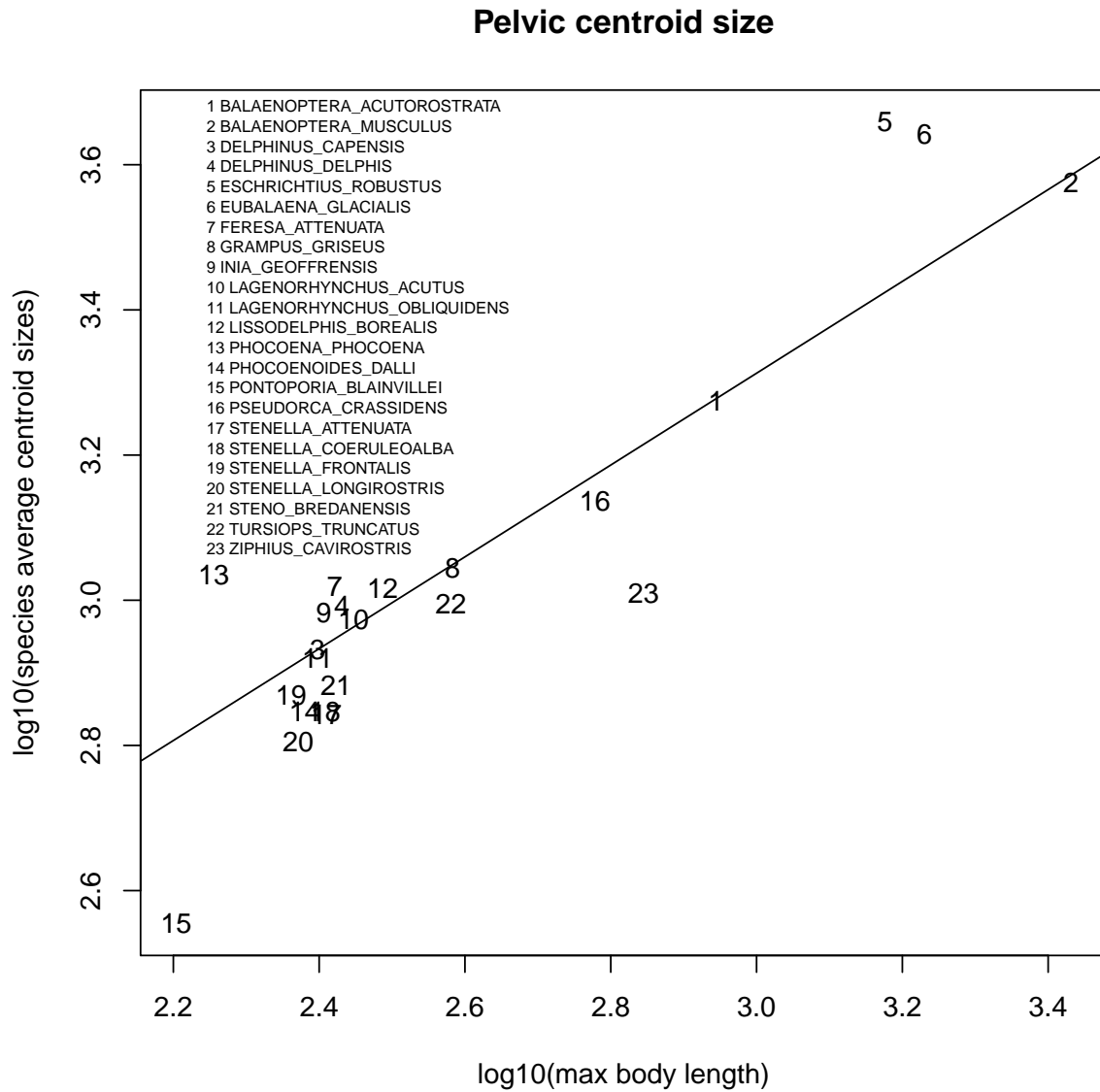


Figure S5. Centroid size onto max body length. For each species (sexually mature males only), an average centroid size was calculated, then regressed onto body length using the gls procedure in the R package nlme, with a correlation structure that accounted for phylogenetic relatedness (44), using the corPagel procedure in the R package ape (45). The phylogenetic residuals of centroid size were used as a measure of relative pelvic size.

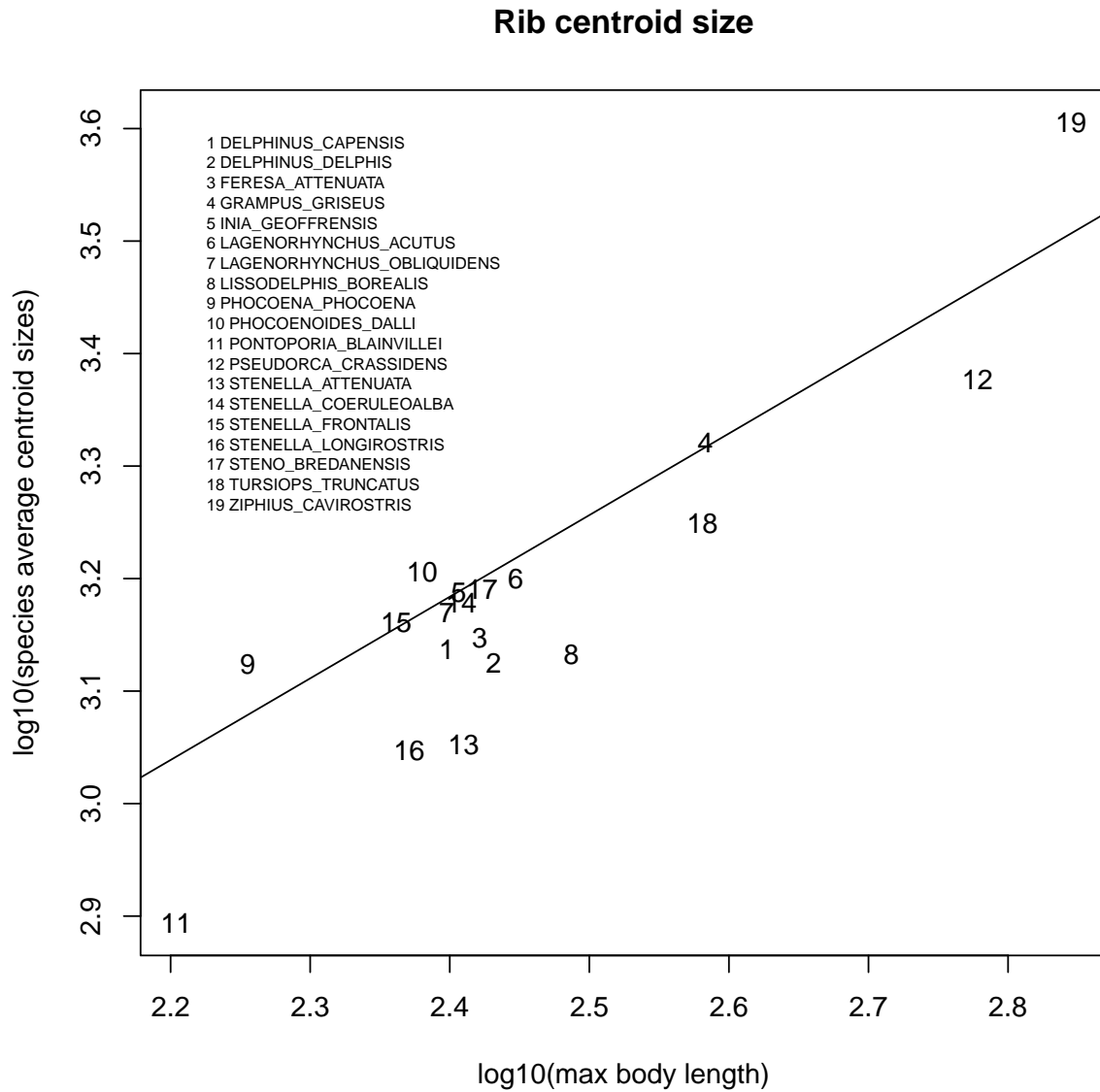


Figure S6. For each species (sexually mature males only), an average rib centroid size was calculated, then regressed onto body length using the gls procedure in the R package nlme, with a correlation structure that accounted for phylogenetic relatedness (44), using the corPagel procedure in the R package ape (45). The phylogenetic residuals of centroid size were used as a measure of relative rib size.

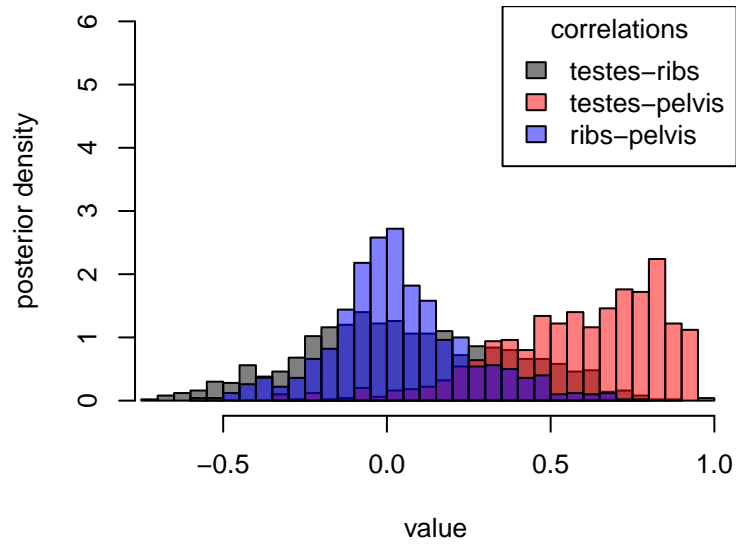


Figure S7. The marginal posterior distributions of correlation coefficients do not change when restricting to bones from adult male cetaceans for which we have both data for both ribs and pelvic bones, which excludes baleen whales. (compare to figure 4 of the main text).

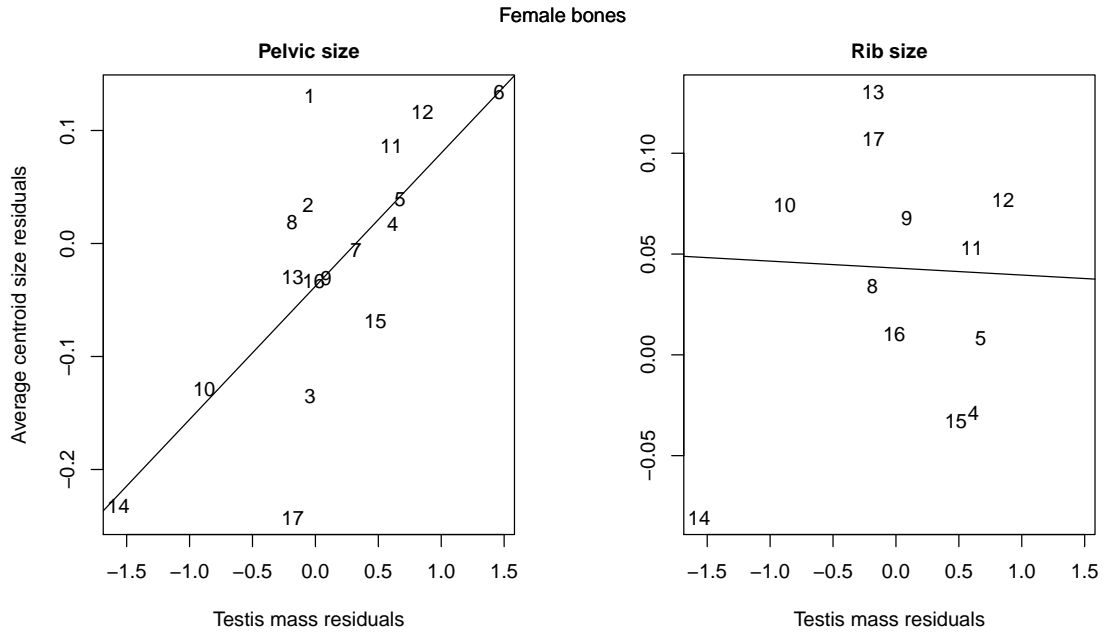


Figure S8. As in males (see Fig. 3 of manuscript), among sexually mature females, residual centroid size (species-average centroid size regressed onto body length) was positively correlated with residual testes mass of males from their species (maximum species testes mass regressed onto maximum body length) in (A) pelvic bones, but not (B) ribs. Species: 1–*Balaenoptera acutorostrata*, 2–*Balaenoptera musculus*, 3–*Balaenoptera physalus*, 4–*Delphinus capensis*, 5–*Delphinus delphis*, 6–*Eubalaena glacialis*, 7–*Globicephala melas*, 8–*Lagenorhynchus acutus*, 9–*Lagenorhynchus obliquidens*, 10–*Mesoplodon carlhubbsi*, 11–*Peponocephala electra*, 12–*Phocoena phocoena*, 13–*Phocoenoides dalli*, 14–*Pontoporia blainvillei*, 15–*Stenella attenuata*, 16–*Tursiops truncatus*, 17–*Ziphius cavirostris*.

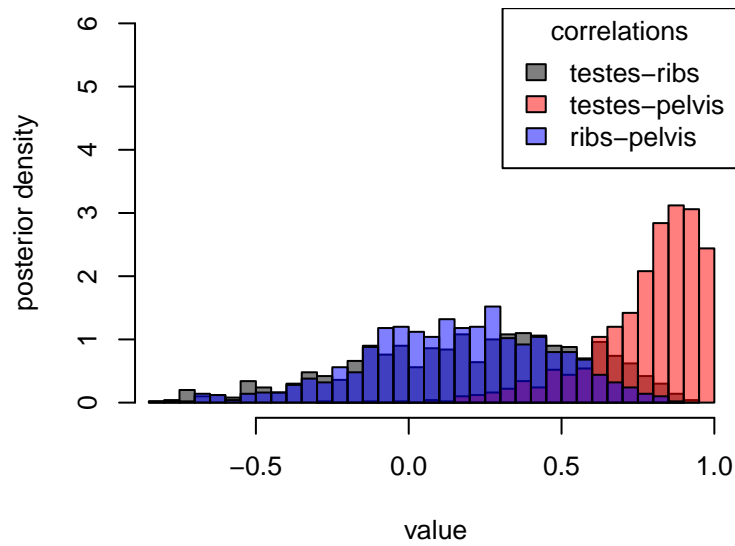


Figure S9. As observed for males (figure 4 of manuscript), the marginal posterior distributions of correlations between changes in female pelvic bone size was significantly correlated with shifts towards larger testis size. Under a phylogenetic model of correlated trait evolution (supplementary methods), the size of the pelvic bone is positively correlated with shifts towards larger testes after accounting for body size evolution (red), while rib bone size does not show this correlation (gray). Only sexually mature females were included in this analysis.

Table S1. Individual level data from bone scans. Only sexually mature individuals included here and in all analyses. NA indicates samples that were absent from museum collection or could not be scanned. Numbers presented for bones are centroid sizes. Museum source indicated in specimen column (BMNH=British Museum of Natural History, CCSN=Cape Cod Stranding Network, LACM=Los Angeles County Natural History Museum, MAL=Marine Animal Life, MH=New England Aquarium, MJM=Michael J. Moore, UMA=University of Massachusetts Amherst, USNM=United States Natural History Museum (Smithsonian), UWBM=University of Washington Burke Museum). Specimens in bold were scanned multiple times to assess technical replication (one juvenile not shown).

| species | specimen | sex | body length | pelvic left | pelvic right | rib left | rib right |
|----------------------------|-------------------|-----|-------------|-------------|--------------|----------|-----------|
| Balaenoptera acutorostrata | MAL_03-282 | F | 730.0 | 2299.8 | 2246.1 | NA | NA |
| Balaenoptera acutorostrata | MH_03-621 | M | 700.0 | 1898.3 | 1868.0 | NA | NA |
| Balaenoptera musculus | BMNH_1953-12.1.18 | F | 2350.0 | 3862.8 | 3771.2 | NA | NA |
| Balaenoptera musculus | BMNH_1953-12.1.19 | M | 2360.0 | 3765.0 | NA | NA | NA |
| Balaenoptera physalus | LACM_31144 | U | 2135.0 | 3648.4 | 3649.3 | NA | NA |
| Balaenoptera physalus | UMA_4820 | F | 2075.0 | 2376.7 | 2405.2 | NA | NA |
| Delphinus capensis | LACM_84071 | M | 209.0 | 860.0 | 858.7 | 1221.3 | 1264.7 |
| Delphinus capensis | LACM_84127 | M | 215.0 | 736.7 | 737.6 | 1222.2 | 1243.3 |
| Delphinus capensis | LACM_84163 | M | 226.0 | 796.7 | 808.0 | 1473.7 | 1458.9 |
| Delphinus capensis | LACM_84185 | M | 211.5 | 907.7 | 898.7 | 1276.7 | 1346.0 |
| Delphinus capensis | LACM_84220 | M | 212.0 | 851.6 | 870.7 | 1361.0 | 1347.5 |
| Delphinus capensis | LACM_84221 | M | 218.5 | 853.1 | 840.8 | 1418.8 | 1442.4 |
| Delphinus capensis | LACM_84233 | M | 223.5 | 963.6 | 943.7 | 1280.4 | 1302.6 |
| Delphinus capensis | LACM_84236 | F | 208.0 | 677.1 | 695.4 | 1210.3 | 1227.1 |
| Delphinus capensis | LACM_84239 | M | 208.5 | 670.5 | 657.6 | 1356.7 | 1357.9 |
| Delphinus capensis | LACM_84240 | M | 235.0 | 884.6 | 868.9 | 1420.8 | 1429.1 |
| Delphinus capensis | LACM_84241 | M | 232.9 | 892.4 | 937.8 | NA | NA |
| Delphinus capensis | LACM_85995 | M | 210.0 | 896.8 | 894.2 | 1463.8 | 1429.0 |
| Delphinus capensis | LACM_86004 | M | 233.0 | 853.4 | 892.7 | 1454.6 | 1450.5 |
| Delphinus capensis | LACM_88979 | M | 211.5 | 902.6 | 903.3 | 1293.9 | 1297.8 |
| Delphinus capensis | LACM_88999 | M | 214.0 | 730.3 | 735.1 | NA | NA |
| Delphinus capensis | LACM_91307 | F | 207.0 | 915.7 | 906.7 | 1270.0 | 1271.4 |
| Delphinus capensis | LACM_91779 | M | 234.0 | 854.5 | 860.3 | 1306.3 | 1289.7 |
| Delphinus capensis | LACM_91915 | M | 222.0 | 895.8 | 928.2 | 1345.6 | 1360.4 |
| Delphinus capensis | LACM_92071 | M | 227.0 | 939.3 | 947.4 | 1454.0 | 1518.5 |
| Delphinus capensis | LACM_92077 | M | 222.5 | 987.2 | 1021.4 | 1342.3 | 1433.3 |

Continued on next page

Table S1 – Continued from previous page

| species | specimen | sex | body length | pelvic left | pelvic right | rib left | rib right |
|----------------------------|-------------------|-----|-------------|-------------|--------------|----------|-----------|
| Delphinus capensis | LACM_95668 | M | 218.0 | NA | NA | 1271.4 | 1241.8 |
| Delphinus capensis | LACM_96366 | M | 217.5 | 860.1 | 825.2 | 1382.1 | 1351.8 |
| Delphinus capensis | LACM_97203 | M | 219.0 | NA | 653.3 | NA | NA |
| Delphinus capensis | LACM_97204 | M | 224.0 | 807.2 | 838.9 | NA | NA |
| Delphinus capensis | LACM_97429 | M | 232.0 | 987.3 | 956.3 | 1477.3 | 1506.3 |
| Delphinus capensis | LACM_97478 | M | 212.0 | 851.8 | 855.3 | 1460.5 | 1455.7 |
| Delphinus delphis | LACM_84254 | M | 229.0 | 938.2 | 915.4 | 1395.5 | 1391.7 |
| Delphinus delphis | USNM_504107 | M | 209.0 | 989.3 | 996.2 | 1379.4 | 706.2 |
| Delphinus delphis | USNM_572632 | M | 223.0 | 870.3 | 852.7 | NA | 1357.1 |
| Delphinus delphis | USNM_572775 | M | 203.0 | 1097.2 | 1097.6 | 1361.3 | 1434.8 |
| Delphinus delphis | USNM_572776 | M | 228.0 | 983.2 | 991.2 | 1388.7 | 1388.4 |
| Delphinus delphis | USNM_572777 | M | 216.0 | 922.4 | 924.3 | 1305.4 | 1426.2 |
| Delphinus delphis | USNM_572859 | F | 207.0 | 820.8 | 839.3 | 1357.6 | 1347.0 |
| Delphinus delphis | USNM_572871 | M | 229.0 | NA | 1051.0 | 1311.3 | 1283.7 |
| Delphinus delphis | USNM_572980 | M | 225.0 | 1028.1 | 1016.2 | 1449.1 | 1387.5 |
| Eschrichtius robustus | UWBM_35430 | M | 1293.0 | 4557.0 | NA | NA | NA |
| Eubalaena glacialis | MJM_070110 | M | 1370.0 | 4305.6 | 4471.8 | NA | NA |
| Eubalaena glacialis | UMA_4920 | F | 1370.0 | 3432.7 | 3395.9 | NA | NA |
| Feresa attenuata | LACM_84252 | M | 214.0 | 1082.9 | 1090.3 | 1334.6 | 1345.3 |
| Feresa attenuata | USNM_550389 | M | 212.0 | 1049.2 | 1049.8 | NA | 1351.9 |
| Feresa attenuata | USNM_571268 | M | 230.0 | 993.6 | 1001.5 | 1517.2 | 1522.4 |
| Globicephala melas | CCSN_04-141 | F | 460.0 | 1306.4 | 1175.8 | NA | NA |
| Grampus griseus | LACM_72546 | M | 360.7 | 1208.7 | 1192.7 | 2347.2 | 2380.0 |
| Grampus griseus | USNM_504126 | M | 298.0 | 1125.2 | 1107.5 | 1976.2 | 2007.2 |
| Grampus griseus | USNM_550391 | M | 286.0 | 988.5 | 1020.2 | 1926.1 | 1922.7 |
| Inia geoffrensis | LACM_19590 | M | 240.0 | 988.5 | 1013.9 | 1462.4 | 1493.0 |
| Inia geoffrensis | LACM_27074 | M | 228.0 | 940.7 | 898.0 | 1567.9 | 1641.4 |
| Lagenorhynchus acutus | USNM_504154 | F | 234.5 | 860.0 | 853.9 | 1580.8 | 1562.2 |
| Lagenorhynchus acutus | USNM_550995 | M | 253.0 | 959.1 | 995.1 | 1618.7 | 1610.3 |
| Lagenorhynchus acutus | USNM_571327 | M | 253.0 | 843.3 | 907.9 | 1578.4 | 1588.3 |
| Lagenorhynchus acutus | USNM_571390 | M | 242.0 | 968.0 | 978.3 | 1550.5 | 1566.8 |
| Lagenorhynchus obliquidens | LACM_84284 | M | 220.0 | 902.3 | 967.9 | 1572.0 | 1517.1 |
| Lagenorhynchus obliquidens | LACM_88951 | M | 192.0 | 885.5 | 856.2 | 1528.5 | 1465.4 |
| Lagenorhynchus obliquidens | LACM_88987 | M | 207.0 | 771.8 | 778.0 | 1475.7 | 1454.0 |
| Lagenorhynchus obliquidens | LACM_92062 | M | 194.0 | 733.2 | 757.2 | 1386.8 | 1417.4 |
| Lagenorhynchus obliquidens | LACM_95514 | F | 223.0 | 765.2 | 717.1 | 1588.5 | 1686.0 |
| Lissodelphis borealis | LACM_72455 | M | 264.4 | 999.8 | 1010.6 | 1343.2 | 1358.5 |

Continued on next page

Table S1 – *Continued from previous page*

| species | specimen | sex | body length | pelvic left | pelvic right | rib left | rib right |
|------------------------|-------------------|-----|-------------|-------------|--------------|----------|-----------|
| Lissodelphis borealis | LACM_95689 | M | 217.8 | 974.3 | 987.5 | 1161.6 | 1245.6 |
| Lissodelphis borealis | USNM_484929 | M | 265.3 | 1128.5 | 1139.6 | 1489.9 | 1536.7 |
| Mesoplodon carlhubbsi | USNM_504128 | F | 532.0 | 1007.1 | 1043.3 | 3119.4 | 3124.1 |
| Peponocephala electra | LACM_54090 | F | 231.0 | 1008.1 | 974.6 | 1611.4 | 1635.9 |
| Phocoena phocoena | LACM_72591 | M | 148.0 | 1063.1 | 1058.3 | NA | NA |
| Phocoena phocoena | LACM_84072 | M | 154.0 | 1018.1 | 995.4 | 1491.8 | 1475.3 |
| Phocoena phocoena | LACM_84073 | F | 173.0 | 829.5 | 872.4 | 1403.8 | 1414.0 |
| Phocoena phocoena | LACM_84076 | F | 178.0 | 945.3 | 997.7 | 1409.8 | 1415.6 |
| Phocoena phocoena | LACM_84086 | F | 164.5 | 880.5 | 877.0 | 1319.0 | 1317.5 |
| Phocoena phocoena | USNM_504302 | F | 165.0 | 834.4 | 917.4 | 1275.9 | 1279.1 |
| Phocoena phocoena | USNM_550042 | U | 149.0 | 1161.8 | NA | 1335.7 | 1316.9 |
| Phocoena phocoena | USNM_550312 | F | 158.0 | 897.4 | 879.9 | 1334.4 | 1362.6 |
| Phocoena phocoena | USNM_571709 | M | 160.2 | 1155.7 | 1159.7 | 1409.4 | 1352.6 |
| Phocoena phocoena | USNM_571723 | M | 146.1 | 1094.4 | 1086.9 | 1125.8 | 1152.4 |
| Phocoena phocoena | USNM_572629 | F | 163.0 | 718.3 | 775.9 | 1361.7 | 1374.8 |
| Phocoena phocoena | USNM_572785 | M | 151.5 | 1108.1 | 1110.9 | 1299.1 | 1328.9 |
| Phocoenoides dalli | LACM_54420 | M | 203.0 | 793.8 | 846.7 | 1679.6 | 1600.2 |
| Phocoenoides dalli | LACM_54569 | F | 200.0 | 690.3 | 695.7 | 1748.3 | 1747.2 |
| Phocoenoides dalli | LACM_84048 | M | 213.0 | 590.0 | 575.1 | 1568.3 | 1510.1 |
| Phocoenoides dalli | LACM_84251 | M | 225.0 | 686.9 | 733.8 | 1749.3 | 1753.2 |
| Phocoenoides dalli | LACM_96383 | M | 213.5 | 770.1 | 777.2 | 1556.0 | 1514.2 |
| Phocoenoides dalli | LACM_96487 | M | 210.0 | 557.9 | NA | NA | NA |
| Phocoenoides dalli | LACM_97207 | M | 210.0 | 691.5 | 677.9 | NA | NA |
| Phocoenoides dalli | USNM_396304 | M | 202.0 | 795.3 | 794.9 | 1567.3 | 1566.4 |
| Pontoporia blainvillei | LACM_47143 | M | 128.5 | 302.0 | 297.5 | 774.5 | 803.6 |
| Pontoporia blainvillei | LACM_54012 | F | 138.0 | 396.6 | 364.7 | 848.7 | 861.0 |
| Pontoporia blainvillei | USNM_501157 | F | 136.0 | 343.5 | 325.3 | 833.2 | 842.3 |
| Pontoporia blainvillei | USNM_501172 | M | 137.0 | NA | NA | 720.1 | 764.6 |
| Pontoporia blainvillei | USNM_501176 | F | 142.0 | 340.0 | 343.2 | 798.8 | 846.6 |
| Pontoporia blainvillei | USNM_501179 | M | 142.0 | 407.2 | 428.4 | 797.5 | 834.9 |
| Pontoporia blainvillei | USNM_501183 | F | 145.0 | 285.2 | 295.8 | 828.4 | 883.0 |
| Pontoporia blainvillei | USNM_501186 | F | 143.0 | 355.9 | 288.3 | 793.3 | 794.0 |
| Pontoporia blainvillei | USNM_504920 | F | 155.0 | 490.4 | 443.4 | 880.8 | 911.0 |
| Pseudorca crassidens | LACM_84047 | M | 480.0 | 1379.1 | 1362.4 | 2352.0 | 2415.8 |
| Stenella attenuata | LACM_54043 | M | 195.0 | 651.2 | 628.4 | 1144.1 | 1155.2 |
| Stenella attenuata | LACM_95489 | F | 191.9 | 572.8 | 545.6 | 1157.5 | 1170.1 |
| Stenella attenuata | USNM_395277 | F | 175.0 | 646.1 | 643.2 | NA | NA |

Continued on next page

Table S1 – Continued from previous page

| species | specimen | sex | body length | pelvic left | pelvic right | rib left | rib right |
|-----------------------|-------------------|-----|----------------|----------------|-----------------|-------------|--------------|
| Stenella attenuata | USNM_395390 | M | 218.0 | 722.1 | 707.3 | 1112.3 | 1128.2 |
| Stenella attenuata | USNM_395465 | M | 200.0 | 759.0 | 712.4 | 1116.3 | NA |
| Stenella coeruleoalba | USNM_504350 | M | 231.0 | 737.4 | 740.6 | 1473.1 | 1459.4 |
| Stenella coeruleoalba | USNM_504773 | M | 221.7 | 669.9 | 662.8 | 1564.6 | 1532.2 |
| Stenella frontalis | USNM_504758 | M | 201.0 | 742.5 | 736.4 | 1434.6 | 1462.4 |
| Stenella longirostris | LACM_72437 | M | 175.4 | 541.2 | 579.8 | 1009.1 | 975.9 |
| Stenella longirostris | LACM_72438 | M | 177.5 | 651.7 | 664.0 | 1179.8 | 1198.3 |
| Stenella longirostris | USNM_395599 | M | 173.0 | 692.4 | 702.7 | 1161.8 | 1157.9 |
| Steno bredanensis | USNM_504467 | M | 235.0 | 737.0 | 761.0 | NA | 1672.7 |
| Steno bredanensis | USNM_504468 | M | 227.0 | 745.8 | 741.6 | NA | 1628.7 |
| Steno bredanensis | USNM_504494 | M | 233.0 | 748.6 | 818.3 | NA | 1393.5 |
| Steno bredanensis | USNM_550837 | M | 228.1 | 787.4 | 780.2 | 1538.6 | 1488.7 |
| Tursiops aduncus | USNM_258642 | M | 287.0 | 905.2 | 914.7 | 1900.4 | 1927.8 |
| Tursiops truncatus | LACM_84194 | M | 304.0 | 1108.3 | 1156.8 | 1827.2 | 1876.1 |
| Tursiops truncatus | LACM_84267 | M | 305.0 | 865.6 | 868.1 | 1941.6 | 1838.3 |
| Tursiops truncatus | LACM_84271 | F | 285.0 | 663.1 | 616.9 | 1720.5 | 1704.1 |
| Tursiops truncatus | LACM_92072 | M | 288.0 | 746.3 | 717.5 | 1768.1 | 1785.2 |
| Tursiops truncatus | LACM_95828 | M | 293.0 | 959.0 | 939.2 | NA | NA |
| Tursiops truncatus | LACM_97405 | F | 277.0 | 842.1 | 955.1 | 1705.4 | 1709.0 |
| Tursiops truncatus | LACM_97489 | F | 298.0 | 1083.8 | 1045.8 | 1817.7 | 1914.5 |
| Tursiops truncatus | USNM_396165 | M | 303.0 | 796.7 | 876.0 | 1911.5 | NA |
| Tursiops truncatus | USNM_504726 | M | 298.0 | 1068.1 | 1094.0 | 2014.3 | 1940.9 |
| Tursiops truncatus | USNM_504879 | M | 284.0 | 1000.5 | 1000.5 | NA | 1874.6 |
| Tursiops truncatus | USNM_550401 | M | 267.5 | 1073.7 | 1046.9 | 1701.2 | 1697.5 |
| Tursiops truncatus | USNM_550422 | M | 279.0 | 1155.2 | 1150.8 | 1812.2 | 1782.7 |
| Tursiops truncatus | USNM_550919 | F | 283.0 | 953.6 | 966.2 | 1833.0 | 1810.8 |
| Tursiops truncatus | USNM_571051 | M | 277.0 | 999.0 | 1024.7 | 1766.0 | 1763.1 |
| Tursiops truncatus | USNM_571086 | M | 273.0 | 1078.9 | 1030.9 | 1644.9 | 1723.9 |
| Tursiops truncatus | USNM_571388 | F | 285.0 | 790.6 | 830.5 | 1491.6 | 1509.5 |
| Tursiops truncatus | USNM_571521 | M | 271.0 | 659.5 | 669.7 | 1399.0 | 1396.5 |
| Tursiops truncatus | USNM_572949 | M | 265.0 | 1166.0 | 1105.4 | 1697.1 | 1644.7 |
| Tursiops truncatus | USNM_593406 | M | 279.0 | 1167.8 | 1172.6 | 1736.8 | 1770.7 |
| Ziphius cavirostris | USNM_A20971 | F | 589.0 | 854.0 | 828.4 | 3676.2 | 3580.3 |
| Ziphius cavirostris | USNM_A49599 | M | 564.0 | 978.7 | 1067.3 | 4095.2 | 3972.7 |

Table S2. Morphological data gathered from literature for sexually mature males.

| species | max body length | maximum body mass | maximum testes mass | references |
|-----------------------------|--------------------------------|------------------------------|--------------------------------|---|
| Balaena mysticetus | 1800 | 90000000 | 163000.0 | Burns et al. (46) |
| Balaenoptera acutorostrata | 880 | 9200000 | 8800.0 | Tomilin (47) |
| Balaenoptera borealis | 1520 | NA | 16400.0 | Perry et al. (48) |
| Balaenoptera edeni | 1500 | 40000000 | 20000.0 | Tomilin (47) |
| Balaenoptera musculus | 2700 | 150000000 | 70000.0 | Tomilin (47) |
| Balaenoptera physalus | 2400 | 90000000 | 58300.0 | Jefferson et al. (49) |
| Caperea marginata | 550 | NA | 1900.0 | Baker (50) |
| Cephalorhynchus commersonii | 174 | 86000 | 930.0 | Goodall (51) |
| Delphinus capensis | 250 | 235000 | 3785.0 | Jefferson et al. (49), Ross (52) |
| Delphinus delphis | 270 | 200000 | 5000.0 | Jefferson et al. (49) |
| Eschrichtius robustus | 1500 | 45000000 | 67500.0 | Tomilin (47) |
| Eubalaena australis | 1700 | 90000000 | 972000.0 | Best et al. (53) |
| Eubalaena glacialis | 1700 | 90000000 | 972000.0 | Best et al. (53) |
| Feresa attenuata | 264 | 225000 | 754.0 | Jefferson et al. (49) |
| Globicephala macrorhynchus | 700 | 3600000 | 7000.0 | Jefferson et al. (49) |
| Globicephala melas | 670 | 2320000 | 12300.0 | Jefferson et al. (49), Desportes et al. (54) |
| Grampus griseus | 383 | 500000 | 10600.0 | Jefferson et al. (49), Perrin and Reilly (55) |
| Inia geoffrensis | 255 | 207000 | 1600.0 | Jefferson et al. (49), Best and da Silva (56) |
| Kogia breviceps | 425 | 417000 | 10000.0 | Tomilin (47), Blood- worth and Odell (57), Caldwell et al. (58), Ruiz (59) |
| Kogia sima | 270 | 280000 | 2618.0 | Ross (52) |
| Lagenorhynchus acutus | 280 | 235000 | 740.0 | Jefferson et al. (49) |
| Lagenorhynchus obliquidens | 250 | 200000 | 1118.0 | Harrison et al. (60) |
| Lissodelphis borealis | 307 | 115000 | 1410.0 | Harrison et al. (60) |
| Megaptera novaeangliae | 1700 | 40000000 | 4000.0 | Jefferson et al. (49) |
| Mesoplodon carlhubbsi | 540 | 1500000 | 510.0 | Jefferson et al. (49), Mead et al. (61) |
| Monodon monoceros | 480 | 1600000 | NA | Jefferson et al. (49) |
| Neophocaena phocaenoides | 200 | 55000 | 863.0 | Kasuya (62) |

Continued on next page

Table S2 – *Continued from previous page*

| species | max body length | max mass | body mass | testes | references |
|------------------------|--------------------------------|---------------------|----------------------|---------------|--|
| Orcinus orca | 975 | 10000000 | 23100.0 | | Jefferson et al. (49), Ross (52) |
| Peponocephala electra | 278 | 275000 | 4500.0 | | Jefferson et al. (49) |
| Phocoena phocoena | 180 | 61000 | 3515.0 | | Read (63) |
| Phocoenoides dalli | 240 | 200000 | 560.0 | | Jefferson et al. (49) |
| Physeter catodon | 1800 | 57000000 | 12000.0 | | Jefferson et al. (49) |
| Pontoporia blainvillei | 160 | 50000 | 10.8 | | Jefferson et al. (49) |
| Pseudorca crassidens | 600 | 2000000 | 14800.0 | | Jefferson et al. (49) |
| Stenella attenuata | 257 | 120000 | 2896.0 | | Jefferson et al. (49), Hohn et al. (64) |
| Stenella coeruleoalba | 256 | 160000 | 500.0 | | Miyazaki (65) |
| Stenella frontalis | 230 | 140000 | 1210.0 | | Perrin et al. (66) |
| Stenella longirostris | 235 | 82000 | 2708.0 | | Jefferson et al. (49) |
| Steno bredanensis | 265 | 160000 | 2660.0 | | Miyazaki and Perrin (67) |
| Tursiops aduncus | 270 | 230000 | NA | | Wells and Scott (68) |
| Tursiops truncatus | 381 | 650000 | 1966.0 | | Perrin and Reilly (55) |
| Ziphius cavirostris | 700 | 3000000 | 4200.0 | | Omura et al. (69) |

| | σ_L | β_T | β_P | β_R | σ_R | σ_P | ζ_L | ζ_R |
|------|------------|-----------|------------|------------|------------|------------|-----------|-----------|
| 5% | 0.11 | 0.38 | 0.03 | -0.02 | 0.03 | 0.05 | 0.04 | 0.06 |
| 25% | 0.14 | 0.44 | 0.05 | -0.01 | 0.03 | 0.06 | 0.04 | 0.07 |
| mean | 0.55 | 0.55 | 0.07 | 0.00 | 0.04 | 0.07 | 0.04 | 0.07 |
| 75% | 0.51 | 0.61 | 0.08 | 0.01 | 0.05 | 0.07 | 0.05 | 0.07 |
| 95% | 2.28 | 0.88 | 0.11 | 0.03 | 0.06 | 0.09 | 0.05 | 0.08 |
| | ω_R | ζ_P | ω_P | δ_T | δ_R | δ_P | η_R | η_P |
| 5% | 0.04 | 0.10 | 0.01 | 0.08 | 0.09 | 0.05 | 0.02 | -0.00 |
| 25% | 0.04 | 0.11 | 0.02 | 0.27 | 0.11 | 0.08 | 0.03 | 0.01 |
| mean | 0.04 | 0.12 | 0.02 | 1.60 | 0.51 | 0.47 | 0.03 | 0.02 |
| 75% | 0.04 | 0.13 | 0.02 | 3.29 | 0.43 | 0.54 | 0.04 | 0.02 |
| 95% | 0.05 | 0.14 | 0.02 | 4.27 | 2.00 | 1.99 | 0.05 | 0.04 |

Table S3. Posterior means and quantiles of the parameters of the model presented in equations (7) and (8), estimated using only bones from adult males.

| | testes–ribs | testes–pelvis | ribs–pelvis |
|---------|-------------|---------------|-------------|
| Min. | -0.8087000 | 0.0594300 | -0.7689000 |
| 2.5% | -0.5075804 | 0.2476295 | -0.3776489 |
| 1st Qu. | -0.1367000 | 0.5748000 | -0.0833000 |
| Median | 0.0759300 | 0.7001000 | 0.0432000 |
| Mean | 0.0665400 | 0.6682000 | 0.0461500 |
| 3rd Qu. | 0.2769000 | 0.7872000 | 0.1720000 |
| 97.5% | 0.6225153 | 0.9025416 | 0.4816755 |
| Max. | 0.8719000 | 0.9694000 | 0.8116000 |

Table S4. Marginal posterior distributions of correlations, with length fixed, between changes in rib size, pelvic bone size, and testes size, estimated using only bones from adult males.

| | σ_L | β_T | β_P | β_R | σ_R | σ_P | ζ_L | ζ_R |
|------|------------|-----------|-----------|-----------|------------|------------|-----------|-----------|
| 5% | 0.22 | 0.42 | 0.01 | -0.02 | 0.03 | 0.05 | 0.04 | 0.06 |
| 25% | 0.42 | 0.50 | 0.05 | -0.01 | 0.03 | 0.07 | 0.04 | 0.07 |
| mean | 1.08 | 0.63 | 0.08 | 0.00 | 0.04 | 0.10 | 0.04 | 0.07 |
| 75% | 1.74 | 0.71 | 0.11 | 0.01 | 0.05 | 0.12 | 0.05 | 0.07 |
| 95% | 2.07 | 0.98 | 0.17 | 0.03 | 0.06 | 0.16 | 0.05 | 0.08 |

| | ω_R | ζ_P | ω_P | δ_T | δ_R | δ_P | η_R | η_P |
|------|------------|-----------|------------|------------|------------|------------|----------|----------|
| 5% | 0.04 | 0.10 | 0.01 | 1.59 | 0.66 | 0.80 | 0.55 | -0.04 |
| 25% | 0.04 | 0.11 | 0.02 | 1.88 | 0.77 | 1.09 | 0.70 | 0.15 |
| mean | 0.04 | 0.12 | 0.02 | 2.50 | 0.86 | 1.32 | 0.82 | 0.30 |
| 75% | 0.04 | 0.13 | 0.02 | 5.55 | 0.93 | 1.51 | 0.93 | 0.45 |
| 95% | 0.05 | 0.14 | 0.02 | 7.95 | 1.03 | 1.87 | 1.10 | 0.64 |

Table S5. Posterior means and quantiles of the parameters given the dataset consisting only of bones from males for which we have both ribs and pelvic bones.

| | testes–ribs | testes–pelvis | ribs–pelvis |
|---------|-------------|---------------|-------------|
| Min. | -0.7011000 | -0.34740000 | -0.5741000 |
| 2.5% | -0.5280824 | -0.04632722 | -0.3928919 |
| 1st Qu. | -0.1584000 | 0.42580000 | -0.0787800 |
| Median | 0.0371700 | 0.63120000 | 0.0126700 |
| Mean | 0.0605700 | 0.58490000 | 0.0372300 |
| 3rd Qu. | 0.2918000 | 0.78740000 | 0.1450000 |
| 97.5% | 0.6390835 | 0.92448522 | 0.4975437 |
| Max. | 0.8554000 | 0.96980000 | 0.7611000 |

Table S6. Marginal posterior distributions of correlations, with length fixed, between changes in rib size, pelvic bone size, and testes size, given only data for bones in males for which we have both ribs and pelvic bones.

| | σ_L | β_T | β_P | β_R | σ_R | σ_P | ζ_L | ζ_R |
|------|------------|-----------|------------|------------|------------|------------|-----------|-----------|
| 5% | 0.13 | 0.39 | 0.02 | -0.02 | 0.02 | 0.01 | 0.02 | 0.04 |
| 25% | 0.15 | 0.46 | 0.04 | -0.00 | 0.02 | 0.03 | 0.03 | 0.05 |
| mean | 0.18 | 0.54 | 0.06 | 0.01 | 0.03 | 0.04 | 0.03 | 0.06 |
| 75% | 0.20 | 0.60 | 0.07 | 0.02 | 0.04 | 0.05 | 0.03 | 0.06 |
| 95% | 0.25 | 0.76 | 0.10 | 0.03 | 0.06 | 0.07 | 0.04 | 0.08 |
| | ω_R | ζ_P | ω_P | δ_T | δ_R | δ_P | η_R | η_P |
| 5% | 0.01 | 0.11 | 0.03 | 0.07 | 0.74 | 0.30 | -0.16 | -0.55 |
| 25% | 0.01 | 0.13 | 0.03 | 0.98 | 0.88 | 0.47 | 0.26 | 0.28 |
| mean | 0.01 | 0.15 | 0.03 | 1.76 | 0.97 | 0.57 | 0.49 | 1.04 |
| 75% | 0.01 | 0.16 | 0.04 | 2.49 | 1.05 | 0.68 | 0.76 | 1.73 |
| 95% | 0.02 | 0.18 | 0.04 | 3.46 | 1.20 | 0.84 | 1.08 | 2.84 |

Table S7. Posterior means and quantiles of the parameters, for bones from females only.

| | testes–ribs | testes–pelvis | ribs–pelvis |
|---------|-------------|---------------|-------------|
| Min. | -0.8225000 | -0.2529000 | -0.8156000 |
| 2.5% | -0.5799271 | 0.3004328 | -0.4842241 |
| 1st Qu. | -0.0687000 | 0.6983000 | -0.0452200 |
| Median | 0.2468000 | 0.8280000 | 0.1670000 |
| Mean | 0.2027000 | 0.7789000 | 0.1576000 |
| 3rd Qu. | 0.4903000 | 0.9067000 | 0.3738000 |
| 97.5% | 0.7967721 | 0.9914113 | 0.6948937 |
| Max. | 0.9369000 | 0.9998000 | 0.8510000 |

Table S8. Correlations from females: Marginal posterior distributions of correlations, with length fixed, between changes in rib size, pelvic bone size, and testes size, given bones from females only.

| Level | Df | Sums of Sqs | Mean Sqs | F.Model | r^2 | Pr(> F) |
|-----------|-----|-------------|----------|---------|-------|---------|
| species | 27 | 258.14 | 9.56 | 945.02 | 0.81 | 0.00 |
| sex | 15 | 27.20 | 1.81 | 179.25 | 0.08 | 0.00 |
| specimen | 89 | 33.68 | 0.38 | 37.40 | 0.11 | 0.00 |
| Residuals | 126 | 1.27 | 0.01 | 0.00 | | |
| Total | 257 | 320.30 | 1.00 | | | |

Table S9. Distance-based ANOVA of pairwise differences in pelvic bone centroid size.

Results from a nested ANOVA performed on the pairwise distance matrix of relative centroid size (centroid size divided by body length). Significance determined with 10,000 permutations, implemented as

“adonis(**distance_matrix** ~ species + sex_within_species + specimen_within_sex_within_species)” in the ADONIS function of the Oksanen et al. (70) package in R.

| Level | Df | Sums of Sqs | Mean Sqs | F.Model | r^2 | Pr(> F) |
|-----------|-----|-------------|----------|---------|-------|---------|
| species | 21 | 141.95 | 6.76 | 103.64 | 0.78 | 0.00 |
| sex | 11 | 6.69 | 0.61 | 9.33 | 0.04 | 0.00 |
| specimen | 82 | 26.07 | 0.32 | 4.88 | 0.14 | 0.00 |
| Residuals | 107 | 6.98 | 0.07 | 0.04 | | |
| Total | 221 | 181.69 | 1.00 | | | |

Table S10. Distance-based ANOVA of pairwise differences in rib bone centroid size. Analysis as described in Table S9.

| Level | Df | Sums of Sqs | Mean Sqs | F.Model | r^2 | $\Pr(> F)$ |
|-----------|-----|-------------|----------|---------|-------|------------|
| species | 27 | 0.18 | 0.01 | 15.57 | 0.34 | 0.00 |
| sex | 15 | 0.07 | 0.00 | 11.18 | 0.14 | 0.00 |
| specimen | 89 | 0.21 | 0.00 | 5.78 | 0.42 | 0.00 |
| Residuals | 126 | 0.05 | 0.00 | 0.10 | | |
| Total | 257 | 0.51 | 1.00 | | | |

Table S11. Distance-based ANOVA of pairwise differences in pelvic bone shape. Analysis as described in Table S9.

| Level | Df | Sums of Sqs | Mean Sqs | F.Model | r^2 | Pr(> F) |
|-----------|-----|-------------|----------|---------|-------|---------|
| species | 21 | 0.09 | 0.00 | 18.72 | 0.45 | 0.00 |
| sex | 11 | 0.01 | 0.00 | 4.93 | 0.06 | 0.00 |
| specimen | 82 | 0.07 | 0.00 | 3.83 | 0.36 | 0.00 |
| Residuals | 107 | 0.02 | 0.00 | 0.12 | | |
| Total | 221 | 0.20 | 1.00 | | | |

Table S12. Distance-based ANOVA of pairwise differences in rib bone shape. Analysis as described in Table S9.

References

- [1] Mark D. Uhen. The origin(s) of whales. *Annual Review of Earth and Planetary Science*, 38: 189–219, 2010.
- [2] W.F. Perrin. World cetacea database (<http://www.marinespecies.org/cetacea>), 2013.
- [3] H.v.W. Schulte and M.F. Smith. The external characters, skeletal muscles and peripheral nerves of *Kogia breviceps*. *Bulletin of the American Museum of Natural History*, 38:7–72, 1918.
- [4] D Pabst, S. A. Rommel, and W. A. Mclellan. Evolution of thermoregulatory function in cetacean reproductive systems. In J. G. M. Thewissen, editor, *The Emergence of Whales: Evolutionary Patterns in the Origin of Cetacea*, pages 379–390. Plenum, New York, 1998.
- [5] Alexander Meek. The reproductive organs of cetacea. *Journal of Anatomy*, 52:186–210, 1918.
- [6] Bruce Mate, Peter Duley, Barbara Lagerquist, Frederick Wenzel, Alison Stimpert, and Phil Clapham. Observations of a female North Atlantic right whale (*Eubalaena glacialis*) in simultaneous copulation with two males: supporting evidence for sperm competition. *Aquatic Mammals*, 31 (2):157–160, 2005.
- [7] R. L. Brownell Jr. and K. Ralls. Potential for sperm competition in baleen whales. *Rep. Int. Whal. Commn.*, 8:97–112, 1986.
- [8] John L. Fitzpatrick, Maria Almbro, Alejandro Gonzalez-Voyer, Niclas Kolm, and Leigh W. Simmons. Male contest competition and the coevolution of weaponry and testes in pinnipeds. *Evolution*, 66(11):3595–3604, 2012.
- [9] S. A. Ramm, G. A. Parker, and P. Stockley. Sperm competition and the evolution of male reproductive anatomy in rodents. *Proc Biol Sci*, 272(1566):949–55, 2005.
- [10] R. C. Firman and L. W. Simmons. The frequency of multiple paternity predicts variation in testes size among island populations of house mice. *J Evol Biol*, 21:1524–1533, 2008.
- [11] G. J. Kenagy and S. C. Trombulak. Size and function of mammalian testes in relation to body size. *Journal of Mammalogy*, 67:1–22, 1986.
- [12] A. P. Møller. Ejaculate quality, testes size and sperm production in mammals. *Functional Ecology*, 3(1):91–96, 1989.
- [13] A. H. Harcourt, P. H. Harvey, S. G. Larson, and R. V. Short. Testis weight, body weight and breeding system in primates. *Nature*, 293(5827):55–7, 1981.
- [14] P. Stockley, M. J. G. Gage, G. A. Parker, and A. P. Moller. Sperm competition in fishes: the evolution of testis size and ejaculate characteristics. *The American Naturalist*, 149(5):933–954, 1997.

- [15] Matthew J. G. Gage. Associations between body size, mating pattern, testis size and sperm lengths across butterflies. *Proceedings of the Royal Society of London. Series B: Biological Sciences*, 258 (1353):247–254, 1994.
- [16] D. J. Hosken. Experimental evidence for testis size evolution via sperm competition. *Ecol. Lett.*, 4:10–13, 2001.
- [17] Online supplementary material.
- [18] D Danilewicz, JA Claver, AL Prez Carrera, ER Secchi, and NF Fontoura. Reproductive biology of male franciscanas (*Pontoporia blainvillei*) (Mammalia: Cetacea) from Rio Grande do Sul, southern Brazil. *Fishery Bulletin*, 102(4):581–592, 2004.
- [19] M. R. McGowen, M. Spaulding, and J. Gatesy. Divergence date estimation and a comprehensive molecular tree of extant cetaceans. *Mol Phylogenet Evol*, 53(3):891–906, 2009.
- [20] Liam J. Revell and David C. Collar. Phylogenetic analysis of the evolutionary correlation using likelihood. *Evolution*, 63:1090–1100, 2009.
- [21] J. E. Heyning and W. F. Perrin. Evidence for two species of common dolphins (genus *Delphinus*) from the eastern north Pacific. *Contributions in Science*, 1994.
- [22] F. J. Rohlf and F. L. Bookstein. *Proceedings of the Michigan Morphometrics Workshop*. University of Michigan Museum of Zoology, Ann Arbor, 1990.
- [23] D.E. Slice. Geometrics morphometrics. *Annual Review of Anthropology*, 36:261–281, 2007.
- [24] D. C. Adams and E. Otárola-Castillo. Package ‘geomorph’: Geometric morphometric analysis of 2d/3d landmark data. R package version 1.0. the comprehensive r network (cran). 2012.
- [25] F. J. Bookstein. Landmark methods for forms without landmarks: morphometrics of group differences in outline shape. *Medical Image Analysis*, 1:225–243, 1997.
- [26] F. L. Bookstein. Biometrics, biomathematics and the morphometric synthesis. *Bulletin of Mathematical Biology*, 58:313–365, 1996.
- [27] P. Mitteroecker and P. Gunz. Advances in geometric morphometrics. *Evolutionary Biology*, 36: 235–247, 2009.
- [28] P. Gunz, P. Mitteroecker, and F. Bookstein. Semilandmarks in three dimensions. In Dennis E Slice, editor, *Modern morphometrics in physical anthropology*, pages 73–98. 2005.
- [29] Brian H. McArdle and Marti J. Anderson. Fitting multivariate models to community data: a comment on distance-based redundancy analysis. *Ecology*, 82(1):290–297, 2001.
- [30] P. J. H. van Bree. On the length and weight of the pelvic bones in the harbour porpoise, *Phocoena phocoena* (Linnaeus, 1758) in relation to sex and size. *Lutra*, 15:8–12, 1973.

- [31] D. Andersen, C. C. Kinze, and J. Skov. The use of pelvic bones in the harbour porpoise *Phocoena phocoena* as an indication of sexual maturity. *Lutra*, 35:105–112, 1992.
- [32] W.F. Perrin. *Variation of spotted and spinner porpoise (genus Stenella) in the Eastern Tropical Pacific and Hawaii*. University of California Press, 1975.
- [33] W. G. Eberhard. *Sexual selection and animal genitalia*. Harvard University Press, Cambridge, Mass., 1985.
- [34] Goran Arnqvist. Comparative evidence for the evolution of genitalia by sexual selection. *Nature*, 393(6687):784–786, 1998.
- [35] D.J. Hosken and P. Stockley. Sexual selection and genital evolution. *Trends in Ecology & Evolution*, 19(2):87–93, 2004.
- [36] Steven A. Ramm. Sexual selection and genital evolution in mammals: a phylogenetic analysis of baculum length. *The American Naturalist*, 169(3):360–369, 2007.
- [37] Liam J. Revell and David C. Collar. Phylogenetic analysis of the evolutionary correlation using likelihood. *Evolution*, 63(4):1090–1100, 2009. ISSN 1558-5646. doi: 10.1111/j.1558-5646.2009.00616.x. URL <http://dx.doi.org/10.1111/j.1558-5646.2009.00616.x>.
- [38] L J Harmon, J T Weir, C D Brock, R E Glor, and W Challenger. GEIGER: investigating evolutionary radiations. *Bioinformatics*, 24(1):129–131, January 2008. doi: 10.1093/bioinformatics/btm538. URL <http://www.ncbi.nlm.nih.gov/pubmed/18006550>.
- [39] John P. Huelsenbeck and Bruce Rannala. Detecting correlation between characters in a comparative analysis with uncertain phylogeny. *Evolution*, 57(6):1237–1247, 2003. ISSN 1558-5646. doi: 10.1111/j.0014-3820.2003.tb00332.x. URL <http://dx.doi.org/10.1111/j.0014-3820.2003.tb00332.x>.
- [40] M Pourahmadi. Joint mean-covariance models with applications to longitudinal data: unconstrained parameterisation. *Biometrika*, 86(3):677–690, 1999. doi: 10.1093/biomet/86.3.677. URL <http://biomet.oxfordjournals.org/content/86/3/677.abstract>.
- [41] J Felsenstein. Maximum-likelihood estimation of evolutionary trees from continuous characters. *Am J Hum Genet*, 25(5):471–492, September 1973. URL <http://www.ncbi.nlm.nih.gov/pmc/articles/PMC1762641/>.
- [42] Charles J. Geyer and Leif T. Johnson. *mcmc: Markov Chain Monte Carlo*, 2013. URL <http://CRAN.R-project.org/package=mcmc>. R package version 0.9-2.
- [43] R Core Team. *R: A Language and Environment for Statistical Computing*. R Foundation for Statistical Computing, Vienna, Austria, 2013. URL <http://www.R-project.org/>.
- [44] M. Pagel. Inferring the historical patterns of biological evolution. *Nature*, 401(6756):877–84, 1999.

- [45] Emmanuel Paradis, Julien Claude, and Korbinian Strimmer. Ape: Analyses of phylogenetics and evolution in R language. *Bioinformatics*, 20(2):289–290, 2004.
- [46] John J. Burns, J. Jerome Montague, and Cleveland A. Cowles. *The Bowhead Whale*. Special Publications of the Society for Marine Mammalogy. Society for Marine Mammalogy, 1993.
- [47] A. G. Tomilin. *Mammals of the USSR and adjacent countries, Vol. 9, Cetacea*. Israel Program for Scientific Translations., Jerusalem, 1967.
- [48] Simona L Perry, Douglas P DeMaster, and Gregory K Silber. The great whales: history and status of six species listed as endangered under the US Endangered Species Act of 1973. *Marine Fisheries Review*, 61(1):1–74, 1999.
- [49] Thomas A. Jefferson, Marc A. Webber, and Robert L. Pitman. *Marine mammals of the world: a comprehensive guide to their identification*. Academic Press, 2008.
- [50] A. N. Baker. Pygmy right whale *Caperea marginata* (Gray, 1846). In S. H. Ridgway and R. Harrison, editors, *Handbook of Marine Mammals, Vol. 3: The Sirenians and Baleen Whales*, pages 345–353. Academic Press, 1985.
- [51] R. N. P. Goodall. Commerson’s dolphin *Cephalorhynchus commersonii* (Lacepede, 1804). In S. H. Ridgway and R. Harrison, editors, *Handbook of Marine Mammals, Vol 5: The First Book of Dolphins*, pages 241–267. Academic Press, 1994.
- [52] G. J. B. Ross. Records of pygmy and dwarf sperm whales, genus *Kogia*, from southern Africa, with biological notes and some comparisons. *Annals of the Cape Provincial Museums Natural History*, 11(14):259–327, 1979.
- [53] P. B. Best, J. L. Bannister, R. L. Brownell, and G. P. Donovan. Right whales: worldwide status. *Journal of Cetacean Research and Management Special Issue*, 2:161–170, 2001.
- [54] Genevieve Desportes, Michael Saboureaux, and Andre Lacroix. Reproductive maturity and seasonality of male long-finned pilot whales, off the Faroe Islands. In *Report of the International Whaling Commission Special Issue (Biology of Northern Hemisphere Pilot Whales)*, volume 4, pages 233–262. 1993.
- [55] William F. Perrin and Stephen B. Reilly. Reproductive parameters of dolphins and small whales of the family Delphinidae, 1984.
- [56] R. C Best and V.M.F. da Silva. Amazon river dolphin, boto *Inia geoffrensis* (de Blainville, 1817). In S. H. Ridgway and R. Harrison, editors, *Handbook of Marine Mammals of the World, Vol. 4: River Dolphins and the Larger Toothed Whales*, pages 1–24. Academic Press, 1989.
- [57] Brian E. Bloodworth and Daniel K. Odell. *Kogia breviceps* (Cetacea: Kogiidae). *Mammalian Species*, 819:1–12, 2008.
- [58] D. K. Caldwell, H. Neuhauser, M. C. Caldwell, and H. W. Coolridge. Recent records of marine mammals from the coasts of georgia and south carolina. *Cetology*, 5:1–12, 1971.

- [59] G. M. Ruiz. *Male reproductive anatomy of the pygmy sperm whale, Kogia breviceps, and the dwarf sperm whale, Kogia simus, based on gross and histological bservations*. Master's thesis, 1993.
- [60] R. J. Harrison, Robert L. Brownell, and R. C. Boice. Reproduction and gonadal appearance in some odontocetes. In R. J. Harrison, editor, *Functional Anatomy of Marine Mammals*, volume 1, pages 361–429. Academic Press, London, 1972.
- [61] J.G. Mead, William A. Walker, and Warren J. Houck. Biological observations on *Mesoplodon carlhubbsi* (Cetacea: Ziphiidae). *Smithsonian Contributions to Zoology*, 344:1–25, 1982.
- [62] T. Kasuya. Finless porpoise *neophocaena phocaenoides* (g. cuvier, 1829). In S. H. Ridgway and R. Harrison, editors, *Handbook of Marine Mammals of the World, Vol. 6: The Second Book of the Dolphins and the Porpoises*, pages 411–442. Academic Press, 1999.
- [63] A.J. Read. Harbour porpoise *Phocoena phocoena* (Linnaeus, 1758). In S. H. Ridgway and R. Harrison, editors, *Handbook of Marine Mammals of the World, Vol. 6: The Second Book of Dolphins and the Porpoises*, pages 323–356. Academic Press, 1999.
- [64] Aleta Hohn, Susan J. Chivers, and Jay Barlow. Reproductive maturity and seasonality of male spotted dolphins, *Stenella attenuata*, in the eastern tropical Pacific. *Marine Mammal Science*, 1(4): 273–293, 1985.
- [65] Nobuyuki Miyazaki. Growth and reproduction of *Stenella coeruleoalba* off the Pacific coast of Japan. *Scientific Reports of the Whales Research Institute Tokyo*, 29:21–48, 1977.
- [66] William F. Perrin, D. K. Caldwell, and M. C. Caldwell. Atlantic spotted dolphin *Stenella frontalis* (G. Cuvier, 1829). In S. H. Ridgway and R. Harrison, editors, *Handbook of Marine Mammals, Vol 5: The First Book of Dolphins*, pages 173–190. Academic Press, 1994.
- [67] Nobuyuki Miyazaki and William F. Perrin. Rough-toothed dolphin *Steno bredanensis* (Lesson, 1828). In S. H. Ridgway and R. Harrison, editors, *Handbook of Marine Mammals, Vol 5: The First Book of Dolphins*, pages 1–21. Academic Press, 1994.
- [68] R. S. Wells and M. D. Scott. Bottlenose dolphin *Tursiops truncatus* (Montagu, 1821). In S. H. Ridgway and R. Harrison, editors, *Handbook of Marine Mammals, vol. 6: The Second Book of Dolphins and Porpoises*, pages 137–182. Academic Press, 1999.
- [69] Hideo Omura, Kazuo Fujino, and Seiji Kimura. Beaked whale *Berardius bairdi* of Japan, with notes on *Ziphius cavirostris*. *Scientific Reports of the Whales Research Institute Tokyo*, 10:89–132, 1955.
- [70] Jari Oksanen, F. Guillaume Blanchet, Roeland Kindt, Pierre Legendre, Peter R. Minchin, R. B. O'Hara, Gavin L. Simpson, Peter Solymos, M. Henry H. Stevens, and Helene Wagner. Package 'vegan': Community ecology. r package version 2.0-7. the comprehensive r network (cran). 2013.